Role of carbon surface diffusion on the growth of epitaxial graphene on SiC

Taisuke Ohta, N. C. Bartelt, Shu Nie, Konrad Thürmer, and G. L. Kellogg
Sandia National Laboratories, Albuquerque, New Mexico 87185, USA
and Sandia National Laboratories, Livermore, California 94550, USA

We have observed the formation of graphene on SiC by Si sublimation in an Ar atmosphere using low-energy electron microscopy, scanning tunneling microcopy, and atomic force microscopy. This work reveals unanticipated growth mechanisms, which depend strongly on the initial surface morphology. Carbon diffusion governs the spatial relationship between SiC decomposition and graphene growth. Isolated bilayer SiC steps generate narrow ribbons of graphene by a distinctive cooperative process, whereas triple bilayer steps allow large graphene sheets to grow by step flow. We demonstrate how graphene quality can be improved by controlling the initial surface morphology to avoid the instabilities inherent in diffusion-limited growth.

PACS number(s): 68.55.−a, 68.35.Fx, 68.37.−d

The unique electronic properties of graphene have stimulated the development of synthesis routes for improved film quality.[1,2] Graphene films form readily on SiC surfaces: sublimation of Si at elevated temperature leaves behind a high concentration of carbon atoms, which assemble ("graphitize") into graphene layers.[3,4] Recent approaches to higher-quality films involve heating in argon at atmospheric pressure[5,6] or supplying excess Si.[7] These new approaches lead to significant improvement in the domain size and electronic properties compared to vacuum graphitization,[8] and call for comprehensive understanding of the kinetic pathways underlying these improvements. The difficulty of studying this system is exacerbated by the relatively high process temperature (>1150 °C), where standard real-time characterization tools are hard to apply. The large number of coexisting intermediate steps and the incompletely characterized surface structures add to the difficulty. Furthermore, the general problem of how new phases form as a surface is depleted of one chemical component during sublimation is not well understood, despite its crucial importance to high-temperature materials processing. Graphene formation on SiC differs from normal epitaxial growth because the constituent atoms are supplied from the substrate itself and are not distributed homogeneously across the surface during the growth. Thus, new fundamental issues, such as how and where carbon atoms are created, and how far they have to diffuse on the surface to form graphene layers, need to be addressed.[9–12]

Here, we report on the initial stages of the first-layer graphene formation on 6H-SiC(0001).[13] Our work establishes the fundamental role of surface diffusion and the importance of the surface morphology in the emergence of a new phase where one or more components are subliming. Our approach is to start with the $(6\sqrt{3} \times 6\sqrt{3})R30°$ carbon-rich termination ("buffer layer")[14–18] made through Ar-assisted graphitization. Because this procedure yields large step-free areas of the buffer layer, the morphology of the surface as graphene grows can be clearly determined. We find that the surface near the growing graphene self-organizes into arrowlike patterns because Si sublimation and graphene growth are spatially connected. We propose that the improvements of the Ar-assisted method are caused by a

changed buffer layer surface morphology, rather than fundamental differences in the mechanism by which graphene forms. As evidence for this we show that large continuous graphene sheets can be grown by vacuum annealing using Ar-assisted buffer layer as a starting substrate.

Figure 1(a) shows the overall surface morphology of the sample surface prepared at 1550 °C in Ar.[19] Almost all steps are found in bunches (indicated by "SB"), which are sepa-
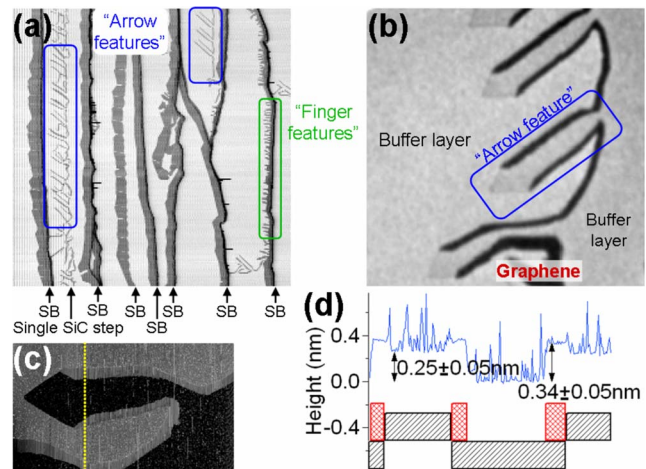
FIG. 1. (Color online) Morphology of SiC surfaces during graphitization. (a) Atomic force microscope (AFM) image (26×26 μm^2) using phase contrast imaging (Ref. 12). Graphene layers (dark gray) are formed at the upper sides (left side in the presented image) of the bunched steps (indicated as SB). A tall bunched step often appears as a black line in an AFM phase image. "Arrow features" and "finger features" are highlighted by the blue and green boxes, respectively. (b) LEEM image of the "arrow features" (4.2×4.2 μm^2) using incident electrons of $E_{vac} + 2.85$ eV, where E_{vac} is the vacuum level. The dark gray regions consist of a graphene monolayer, and the light gray regions are buffer layer. (c) STM image (1.8×1.05 μm^2, tip bias of −2.5 V, and tunneling current of 0.2 nA) with the cross section along the yellow line. (d) Red and black hatched boxes in (d) illustrate a proposed step structure with the cross sections of graphene (1 ML) and buffer layer (0 ML) regions with their thicknesses of 0.33 and 0.25 nm, respectively (Ref. 22).
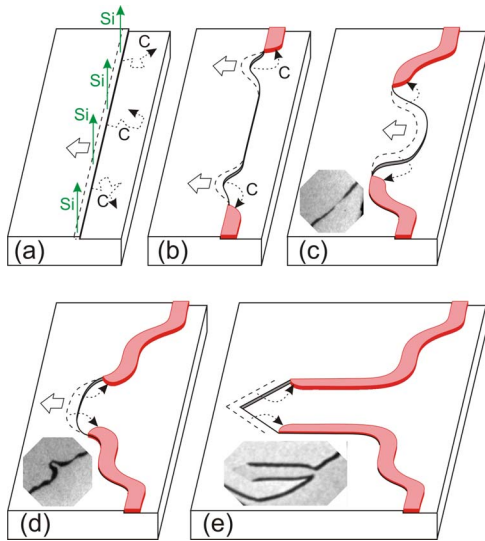
FIG. 2. (Color online) Schematic of the formation of an arrow feature. The insets show static LEEM images of SiC bilayer steps at similar stages of evolution. LEEM images are (c) 2×2 μm^2, (d) 2×2 μm^2, and (e) 4×2 μm^2.

rated by several-micron-wide terraces. The dark gray regions are graphene layers, and the rest of the surface is the buffer layer. Graphene layers are commonly found near the upper sides of the bunched steps. At the single bilayer SiC steps, which occasionally cross the flat terraces, the graphene morphology can be very intricate [see Figs. 1(a) and 1(b)]. Graphene monolayer (ML)-terminated regions, identified using low-energy electron microscopy (LEEM),[8,20] commonly appear as distinctive parallel ribbons [Fig. 1(b)], ending at a triangular arrowhead. As we discuss below the analysis of these "arrow features" provides insights into carbon diffusion. To determine their surface morphology we imaged similarly prepared samples with scanning tunneling microscopy (STM) in ultrahigh vacuum (UHV). As shown in Figs. 1(c) and 1(d), the buffer layer between the parallel ribbons is about $0.35(\pm 0.05)$ nm lower than the graphene ribbons and 0.25 nm lower than the surrounding buffer layer. Considering that the SiC bilayer height is 0.25 nm and that the thickness of graphene is close to the interlayer spacing of graphite, 0.33 nm,[21] we deduce that the graphene layer is formed on top of the buffer layer and decorates the lower side of SiC steps [Fig. 2(e)]. The sides of the ribbon tend to be aligned along [1$\bar{1}$00] (and its equivalent) directions of the SiC substrate.

The relationship between the graphene ribbons and the atomic step configuration of the buffer layer surface suggests the qualitative picture of graphene formation shown in Fig. 2. Starting from a single bilayer SiC step edge on the graphene-free surface, C atoms are emitted onto the terrace [Fig. 2(a)] as Si atoms leave the surface. Eventually these carbon atoms coalesce and nucleate a graphene ribbon at the step edge [Fig. 2(b)]. This graphene ribbon acts as a sink for subsequently emitted C, but also prevents the decorated SiC step from being etched. This poisoning of SiC etching occurs presumably because a fully (σ-)bonded surface of the buffer layer exists across the surface[17] and there is no easy route for

Si atoms to evaporate through the boundary between the graphene ribbon and the buffer layer. STM images show that the $6\sqrt{3}$ surface structure is continuous across this boundary (not shown). Thus, subsequent etching occurs preferentially near the point of contact of the graphene ribbon with the undecorated SiC step, causing the graphene ribbon to be drawn along the etched SiC step [Fig. 2(c)]. Eventually the initial SiC step edge becomes completely decorated by the graphene and etching can only occur if new lengths of SiC steps are created. This step-creation process initiates the formation of a rapidly etching dent in the step edge when two ribbons approach each other [Fig. 2(d)]. This dent develops into the arrowlike features [Fig. 2(e)]. That the etching step edge is oriented in crystallographic directions indicates either that the etching is anisotropic or that the surface mobility along buffer layer steps is large enough for the steps to assume low-energy orientations. Some intermediate states have been detected in static LEEM (insets in Fig. 2) supporting this scenario.

Can this qualitative picture be substantiated by a more rigorous analysis and what does it tell us about the atomic mechanisms of graphene formation? First we note that the areal ratio between the etched buffer layers in the arrow feature and graphene ribbon is 3.0. This ratio is consistent with the C atom conservation: when a SiC step retracts and sweeps through an area A, the number of carbon atoms removed is equal to that required to form an area $A/3.14$ of graphene.[11] Second, that the etched steps are located near graphene suggests that evaporation of Si only occurs if there is a nearby sink of C. As we show next, this implies that the decomposition of SiC at these temperatures is limited by C diffusion.

Consider a sublimating SiC step from which carbon atoms are being emitted onto the adjoining terraces. If the carbon concentration adjacent to the step builds up because of a lack of nearby carbon sinks, Si evaporation will slow and eventually stop assuming the initial evaporation rate is not too large.[23] This is because the increased carbon chemical potential of the dense adatom gas reduces the driving force for Si evaporation (i.e., it reduces the equilibrium Si vapor pressure). In this case the sublimation rate is limited by how fast the carbon diffuses away from the step: suppose that the sublimating step is a distance L from a graphene sheet and c_0 is the carbon concentration where evaporation ceases. The flux f away from the step will then be Dc_0/L and determined by the carbon diffusion constant D. The system will always enter this diffusion-limited regime as L becomes sufficiently large, i.e., when the sublimating step moves far enough away from the graphene sheet.

This diffusion-controlled growth naturally leads to instabilities that prevent graphene growth from proceeding via advancement of straight steps. For example, consider a straight SiC step receding from an initially straight graphene edge. If one region of the graphene sheet gets closer to the etched SiC step from a random fluctuation, it will grow faster, increasing the perturbation and roughening the straight step. It is of considerable interest, as we now show, that the experimentally observed arrow geometry represents a stable steady-state geometry of graphene growing via diffusion-limited etching of SiC steps. For the ribbon to be a
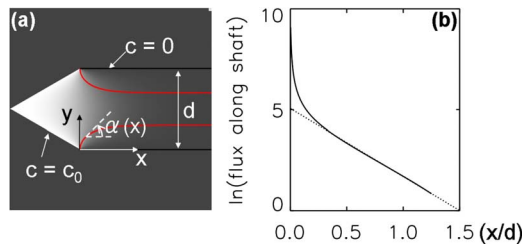
FIG. 3. (Color online) (a) The calculated surface C adatom concentration map derived by solving the time-dependent diffusion equation for the arrow geometry. (b) Profile of the carbon flux along the shaft of the arrow feature.

steady-state geometry, the carbon flux to the sides of the ribbon far from the arrowhead must vanish sufficiently quickly to allow the ribbon to have a fixed asymptotic width. (Otherwise, the ribbon would continue to widen as the SiC step is etched.) To establish that such a steady state exists, we solve the time-dependent diffusion equation for the arrow geometry [Fig. 3(a)]. We suppose that the ribbon is a perfect sink of carbon and thus take $c=0$ along the perimeter of the arrow shaft. We assume that sublimation is diffusion limited and accordingly fix the carbon concentration to be c_0 at the etched steps. Elsewhere, $\nabla^2 c=0$. Figure 3(b) plots the logarithm of the flux as a function of the distance x along the shaft of the arrow. Asymptotically f falls off exponentially with a decay length of $\sim 0.30d$, where d is the width of the arrow. To determine if this functional form, $z(x)$, is consistent with steady-state ribbon growth, we consider a ribbon shape $y(x)$, and for simplicity we assume that y is small compared to d. Since the flux causes graphene growth perpendicular to the step normal, this gives an equation for $y(x,t)$: $\partial y/\partial t=f(x)/\cos(\alpha)=f(x)[1+(\partial y/\partial x)^2]^{1/2}$, where α is the angle between the x axis and the tangent to the graphene step edge. We are looking for steady-state translating solutions of the form $y(x,t)=z(x+vt)$, where v is the arrow etching velocity. If $f(x)=\exp(-x/a)$, then substitution shows that $z(x)=2a\ln\cos(x/2a)$ is such a solution.[24] As shown by the red line in Fig. 3(a) it consists of a ribbon of width a. So at least far from the head of the arrow, where the flux decays exponentially, the ribbon shape represents a steady state. Also, consistent with this model, the observed narrowing of the ribbon near the growing tip extends only to a size comparable to the arrow width.

We have assumed that there is no appreciable barrier for carbon attachment to the graphene edge. If there were a large barrier, the concentration of carbon atoms would be larger far into the shaft of the arrow, causing growth of the ribbon far from the SiC step, which is inconsistent with experiment. Thus, if a barrier exists it is not significant. Graphene growth on SiC (or on buffer layers) appears much different than on metals, where very large barriers to carbon attachment have been reported.[25]

To make a more detailed calculation of the steady-state shape, and in particular to understand what determines the absolute dimension of the arrow, requires a more careful examination of the point where the graphene apex meets the buffer layer step. At this location the C flux to the graphene diverges because the distance between the etching arrowhead
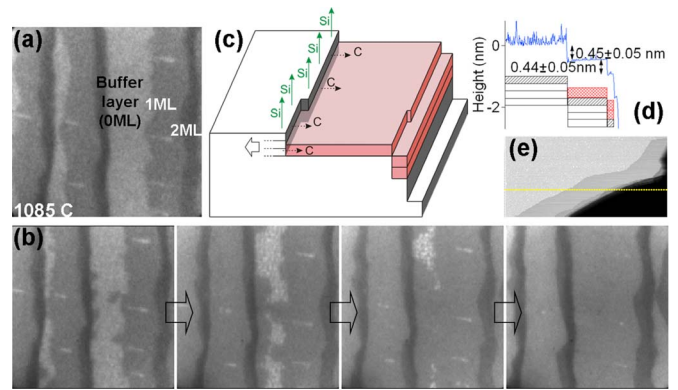
FIG. 4. (Color online) Step flow growth of graphene. (a) and (b) Growth observed in LEEM (3.5×3.5 μm^2). The dark gray regions consist of >2 ML of graphene, the medium gray regions are graphene monolayer, and the light gray regions are buffer layer. (c) Schematic of the step flow. Triple bilayers of SiC (dotted lines) are transformed into a single graphene layer. (d) The cross section of the STM image in (e). The step bunch and the lower terraces are omitted. Red and black hatched boxes and white boxes indicate 1 ML graphene, buffer layer, and SiC bilayer, respectively (Ref. 28). (e) STM image (4×2 μm^2, tip bias of 1.7 V, and tunneling current of 0.1 nA) of the sample with monolayer and bilayer graphene growing from the step bunch.

and the sink vanishes [Fig. 3(b)]. This diverging flux would not allow for a steady-state translating solution. One process which would remove this divergence is the Gibbs-Thomson effect. A graphene edge with radius of curvature R is in equilibrium with an adatom concentration of $c_{eq}\exp[\beta/(kTR\rho)]$, where β is the graphene edge free energy per unit length, c_{eq} is the concentration in equilibrium with a straight graphene edge, and ρ is the number of carbon atoms per unit area of graphene. If R is such that this concentration is approximately equal to c_0, the flux divergence near the contact point is removed. This requirement sets the size of ribbons, thus explaining the uniform arrow width. (The presence of Ar suppresses Si sublimation, reducing c_0 and hence increasing R and the ribbon size.) A complete model would need to consider the orientational anisotropies of the edge energies and the possibility that diffusion of carbon along the edges could be competitive with diffusion on the terraces. Nevertheless, it is clear that the morphology of the growing graphene is determined by how carbon diffuses from the etched SiC bilayer steps to the graphene ribbons.

The relationship among Si sublimation, carbon diffusion, and the graphene growth depends on the step morphology of the buffer layer. Next we show that the role of carbon diffusion is qualitatively different near receding triple bilayer SiC steps. A sequence of LEEM images (using thermionically emitted electrons) of such a step is displayed in Figs. 4(a) and 4(b). Here, the graphene single layer (medium gray) grows into the area covered with buffer layer in a continuous step flow mode, while the sample is annealed from $\sim 1085\ °C$ to $\sim 1200\ °C$ in UHV. Static UHV-STM at room temperature reveals an upward step at the growing front of the graphene: the area covered with graphene appears lower than the adjacent buffer layer by about 0.45 nm [Fig. 4(d)] supporting the LEEM observation. The measured distance of

0.45 nm is reasonably close to the difference in height between three SiC bilayers (0.75 nm=0.25 nm×3) and a graphene monolayer (0.33 nm) as illustrated in Fig. 4(d).[26,27]

Why simple step flow growth can occur in this situation is clear when one considers the carbon balance associated with the etching of the triple bilayer step. The number of carbon atoms emitted per unit area as a triple bilayer step is etched is approximately equal to the number of carbon atoms in the same area of graphene.[11] Thus, the carbon atoms emitted from the step edges can be immediately consumed at the growth front of graphene [Fig. 4(c)]. The graphene formed in step flow growth evidently does not hinder the etching of the triple bilayer SiC steps because SiC bilayer steps are still exposed, allowing Si to directly evaporate. No long-range diffusion of C is necessary in a simple step flow growth mode. Note that the formation of graphene behind a triple bilayer SiC step occurs even during vacuum annealing and does not require an Ar atmosphere. This suggests the Ar atmosphere improves graphene quality not by fundamentally modifying the growth process but instead by removing single bilayer SiC steps on the buffer layer surface by promoting step bunching. A similar improvement can be expected for vicinal SiC substrates.[11]

When the initial step morphology is more complex than isolated single or triple bilayer steps, it becomes more difficult to correlate the etching of a particular step with a particular growth front. We observed a complex finger-shape growth morphology near SiC bilayer steps located near step bunches [Fig. 1(a)] as also shown by others.[9,12]

Our work establishes that the observed distinctive growth morphologies result from cooperative processes caused by Si sublimation rates depending on carbon adatom concentrations. For first-layer graphene growth, we have found that there exist well-defined spatial relationships between where SiC is etched and how and where graphene grows. The spatial relationship is determined by the starting step configuration of the buffer layer surface. The growth of high-quality large-area graphene most likely arises from etching pre-existing triple bilayer SiC steps, where simple step flow is possible. Step flow growth is not possible near etched single bilayer SiC steps because instabilities caused by carbon diffusion lead to complex growth morphologies. Thus, growing better graphene requires minimizing the number of single bilayer SiC steps on the buffer layer surface.

[1] A. K. Geim and K. S. Novoselov, Nature Mater. **6**, 183 (2007).

[2] A. K. Geim, Science **324**, 1530 (2009).

[3] I. Forbeaux, J. M. Themlin, and J. M. Debever, Phys. Rev. B **58**, 16396 (1998).

[4] C. Berger *et al.*, Science **312**, 1191 (2006).

[5] K. V. Emtsev *et al.*, Nature Mater. **8**, 203 (2009).

[6] C. Virojanadara, M. Syväjarvi, R. Yakimova, L. I. Johansson, A. A. Zakharov, and T. Balasubramanian, Phys. Rev. B **78**, 245403 (2008).

[7] R. M. Tromp and J. B. Hannon, Phys. Rev. Lett. **102**, 106104 (2009).

[8] T. Ohta, F. El Gabaly, A. Bostwick, J. L. McChesney, K. V. Emtsev, A. K. Schmid, T. Seyller, K. Horn, and E. Rotenberg, New J. Phys. **10**, 023034 (2008).

[9] V. Borovikov and A. Zangwill, Phys. Rev. B **80**, 121406(R) (2009).

[10] S. W. Poon, W. Chen, E. S. Tok, and A. T. S. Wee, Appl. Phys. Lett. **92**, 104102 (2008).

[11] M. Hupalo, E. H. Conrad, and M. C. Tringides, Phys. Rev. B **80**, 041401(R) (2009).

[12] M. L. Bolen, S. E. Harrison, L. B. Biedermann, and M. A. Capano, Phys. Rev. B **80**, 115433 (2009).

[13] *N* type, ~0.1 Ω cm; Cree, Inc.

[14] W. Chen, H. Xu, L. Liu, X. Gao, D. Qi, G. Peng, S. C. Tan, Y. Feng, K. P. Loh, and A. T. S. Wee, Surf. Sci. **596**, 176 (2005).

[15] A. Mattausch and O. Pankratov, Phys. Rev. Lett. **99**, 076802 (2007).

[16] F. Varchon, R. Feng, J. Hass, X. Li, B. N. Nguyen, C. Naud, P. Mallet, J.-Y. Veuillen, C. Berger, E. H. Conrad, and L. Magaud, Phys. Rev. Lett. **99**, 126805 (2007).

[17] K. V. Emtsev, F. Speck, T. Seyller, L. Ley, and J. D. Riley, Phys. Rev. B **77**, 155303 (2008).

[18] J. Hass, J. E. Millán-Otoya, P. N. First, and E. H. Conrad, Phys. Rev. B **78**, 205424 (2008).

[19] Samples were annealed in a high-temperature furnace at atmospheric pressure with no dwell time at the maximum temperature.

[20] H. Hibino, H. Kageshima, F. Maeda, M. Nagase, Y. Kobayashi, and H. Yamaguchi, Phys. Rev. B **77**, 075413 (2008).

[21] T. Ohta, A. Bostwick, J. L. McChesney, T. Seyller, K. Horn, and E. Rotenberg, Phys. Rev. Lett. **98**, 206802 (2007).

[22] The $6\sqrt{3}$ structure was observed between the spikes in the STM images, suggesting that spikes are due to adsorbed atoms.

[23] J. Tersoff, D. E. Jesson, and W. X. Tang, Science **324**, 236 (2009).

[24] W. W. Mullins, J. Appl. Phys. **27**, 900 (1956).

[25] E. Loginova, N. C. Bartelt, P. J. Feibelman, and K. F. McCarty, New J. Phys. **10**, 093026 (2008).

[26] P. Lauffer, K. V. Emtsev, R. Graupner, T. Seyller, L. Ley, S. A. Reshanov, and H. B. Weber, Phys. Rev. B **77**, 155426 (2008).

[27] The discrepancy of the graphene layer heights between Figs. 1(c) and 4(e) could be caused by different scanning conditions, by the difficulty in determining the relative height of the buffer layer due to impurity atoms, or by the large scanning ranges.

[28] Buffer layer is drawn to have the same height to a SiC bilayer since its thickness is unknown. Our discussion holds for an unknown thickness of buffer layer as it uniformly shifts the surface topography with respect to a SiC substrate.